ChemSusChem

Research Article
doi.org/10.1002/cssc.202301285

Chemistry Europe
European Chemical Societies Publishing

www.chemsuschem.org

Special Collection

Nitrile-functionalized Poly(siloxane) as Electrolytes for High-Energy-Density Solid-State Li Batteries

Faruk Okur,[a, b] Yauhen Sheima,[c] Can Zimmerli,[a, b] Huanyu Zhang,[a, b] Patrick Helbling,[c] Ashling Fäh,[a, b] Iacob Mihail,[c] Jacqueline Tschudin,[c] Dorina M. Opris,*[c, d] Maksym V. Kovalenko,*[a, b] and Kostiantyn V. Kravchyk*[a, b]

In the quest to replace liquid Li-ion electrolytes with safer and non-toxic solid counterparts for Li-ion batteries, polysiloxane polymers have attracted considerable attention as they offer low glass transition temperatures, stability with metallic lithium, and versatility in chemical functionalization of the backbone. Herein, we present the synthesis of Li-ion conductive polysiloxane-based polymers functionalized with 60% nitrile groups per chain unit. The synthesis procedure is based on the reaction of poly-(dimethylsiloxane-*co*-methylvinylsiloxane) polymer with 2-cyanoethanethiol, followed by the addition of lithium bis (trifluoromethanesulfonyl) imide. The presented polysiloxane-based polymers exhibit exceptionally high ionic conductivity up to 0.375 mS cm^{-1} at 60 °C and Li^+ ion transfer number of 0.73, one of the highest reported for polymer Li-ion conducting electrolytes. Their electrochemical performance was evaluated in both symmetrical and full-cell configurations to test the utility of synthesized polymers as electrolytes in Li-ion batteries.

Introduction

Currently, replacing liquid Li-ion electrolytes with their non-flammable and non-toxic solid counterparts based on solid polymers is pursued as a compelling approach to improve the energy density, cycling stability, and safety of Li-ion batteries.[1] The seminal work of Armand *et al.* in 1983,[2] investigating poly (ethylene oxide) complexes with alkali metal salts has since catalyzed a dynamic research landscape that encompasses a diverse array of polymer materials, including polycarbonates,[3] polyphosphazene,[4] and polysiloxanes (PSs).[5] Among these, PS-based solid electrolytes (PSSE) appeal for their compelling set of properties: (i) low glass transition temperature (T_g); due to flexible Si–O–Si bonds, which promote segmental motion of the polymer chain and enable facile ion transfer alongside the polymer network, (ii) high stability with lithium metal anode and (iii) flexibility to chemical modification of the backbone.[5b,6]

However, practical deployment of PSSEs in solid-state Li batteries still faces several challenges. A critical hurdle involves the ion-insulating nature of the polymer backbone, which curtails the efficient transport of lithium ions, resulting in relatively low Li-ion conductivity (< 0.01 mS cm^{-1} at 60 °C).[7] To mitigate this limitation, diverse strategies such as copolymerization,[8] grafting,[9] crosslinking,[10] and blending[11] have been explored.[5b] These approaches introduce polar units into the polymer structure, thereby enhancing the solvation of Li-ions and consequently elevating ionic conductivity. In tandem with incorporating additional polar units, another effective strategy for bolstering Li-ion solvation involves functionalizing the PS backbone with polar CN groups.[12] Initial investigations into the impact of CN groups on PSSE ionic conductivity were carried out by Lee *et al.*[13] The functionalization of cross-linked PS with propilonitrile groups *via* allyl cyanide was found to facilitate ion-pair dissociation, leading to an increase in Li-ion charge carrier concentration and a subsequent enhancement in Li-ion conductivity (to *ca.* 0.138 mS cm^{-1} at 60 °C). Subsequently, our research group[14] demonstrated that functionalizing all PS chains with thiopropionitrile groups using 3-mercaptopropionitrile increases the dielectric permittivity of polysiloxane polymers and hence improves the Li-ion solvation. Nevertheless, a full functionaliza-

[a] F. Okur, C. Zimmerli, H. Zhang, A. Fäh, Prof. M. V. Kovalenko, Dr. K. V. Kravchyk
Laboratory of Inorganic Chemistry, Department of Chemistry and Applied Biosciences
ETH Zurich
CH-8093 Zürich (Switzerland)
E-mail: mvkovalenko@ethz.ch

[b] F. Okur, C. Zimmerli, H. Zhang, A. Fäh, Prof. M. V. Kovalenko, Dr. K. V. Kravchyk
Laboratory for Thin Films and Photovoltaics
Swiss Federal Laboratories for Materials Science & Technology
CH-8600 Dübendorf (Switzerland)
E-mail: kostiantyn.kravchyk@empa.ch

[c] Dr. Y. Sheima, P. Helbling, Dr. I. Mihail, J. Tschudin, Prof. D. M. Opris
Functional Polymers
Swiss Federal Laboratories for Materials Science & Technology
CH-8600 Dübendorf (Switzerland)
E-mail: dorina.opris@empa.ch

[d] Prof. D. M. Opris
Department of Materials
ETH Zurich
CH-8092 Zürich (Switzerland)

Supporting information for this article is available on the WWW under https://doi.org/10.1002/cssc.202301285

Special Collection This publication is part of a joint Special Collection on Solid State Batteries, featuring contributions published in Advanced Energy Materials, Energy Technology, Batteries & Supercaps, ChemSusChem, and Advanced Energy and Sustainability Research.

tion of PS units with CN groups resulted in a notable decrease in ionic conductivity (to *ca.* 0.048 mS cm^{-1} at 60 °C).

Following the initial reports by Lee *et al.*[13] and our recent publication on PSSEs,[14] we sought to continue the evaluation of the content of CN groups in the PS polymer chain on the ionic conductivity of polysiloxane-based polymers. By synthesizing PS polymers with varying CN group contents, our study unveiled that while the incorporation of CN groups boosted dielectric permittivity and thus improved lithium bis-(trifluoromethanesulfonyl) imide (LiTFSI) solvation in the PS polymer, an increase in nitrile group content concurrently led to an increase in T_g, thereby impeding polymer chain mobility. Moreover, we investigated the impact of the CN:Li$^+$ ratio on the ionic conductivity of polysiloxanes. Both factors, i.e., the content of CN groups and the CN:Li ratio, and their effects on the Li-ion conductivity of polysiloxanes, are thoroughly discussed in this work. The practical feasibility of the synthesized polymers for solid-state Li batteries was assessed through a series of measurements, encompassing critical current density, oxidation stability, and galvanostatic cycling in symmetrical-cell (Li/PSSE/Li) and full-cell (Li/PSSE/LFP + PSSE) configurations with a $LiFePO_4$ (LFP) cathode.

Results and Discussion

Preparation and analysis of PSSEs

PSSEs were synthesized according to the procedure shown in Figure 1. First, poly-(dimethylsiloxane-*co*-methylvinylsiloxane) (PM_xV_y) or poly (methylvinylsiloxane) (PV) polymers with different amounts of vinyl groups were dissolved in tetrahydrofuran (THF). Subsequently, they were mixed with 2-cyanoethanethiol and 2,2-dimethoxy-2-phenylacetophenone (DMPA), which served as CN group source and photoinitiator, respectively. The reaction between thiol and vinyl groups resulted in the formation of PS-polymers functionalized with CN groups. The content of vinyl groups was determined based on the molar ratio of repeating units with and without vinyl groups, specifically dimethylsiloxane/methylvinylsiloxane ratios of 6:4; 4:6; 2:8 and 0:1. Considering that *ca.* 5% of the vinyl side groups were subsequently used for crosslinking, the amount of 2-cyanoethanethiol was adjusted to about 0.95 equivalents per vinyl group in PM_xV_y or PV.

To induce Li-ion conductivity, different amounts of LiTFSI salt were dissolved in the synthesized polymers, corresponding to CN:Li$^+$ molar ratios of 20, 15, 10, or 5. DMPA and 2,2′-(ethylenedioxy) diethanethiol were subsequently added to the polymer slurry as the photo-initiator and cross-linker, respectively. The resulting mixture was blade-coated onto a Teflon substrate, followed by UV crosslinking and vacuum drying of the obtained polymer tapes. The prepared electrolytes were denoted as PS–X-Y (Table S1), where X indicates the percentage of the repeating units that are functionalized with CN groups (40, 60, 80, or 100%) and Y refers to the CN:Li$^+$ ratio (20, 15 10 or 5). A detailed description of the synthesis and the preparation of PSSEs can be found in the Experimental Section.

For comprehending the impact of CN content and CN:Li$^+$ ratio on the ionic conductivity of PSSEs, series of electrochemical impedance spectroscopy measurements (EIS) were performed on as-synthesized PS–X–Y compositions. As follows from Figure 2a, comparing the ionic conductivity of PS–X–Y electrolytes containing different content of CN groups and CN:Li$^+$ molar ratios, two correlations were clearly observable. First, as expected, the ionic conductivity increases with the concentration of Li$^+$ ions in the polymer structure (decreasing the CN:Li$^+$ ratio from 20 to 5). Notably, further reduction of

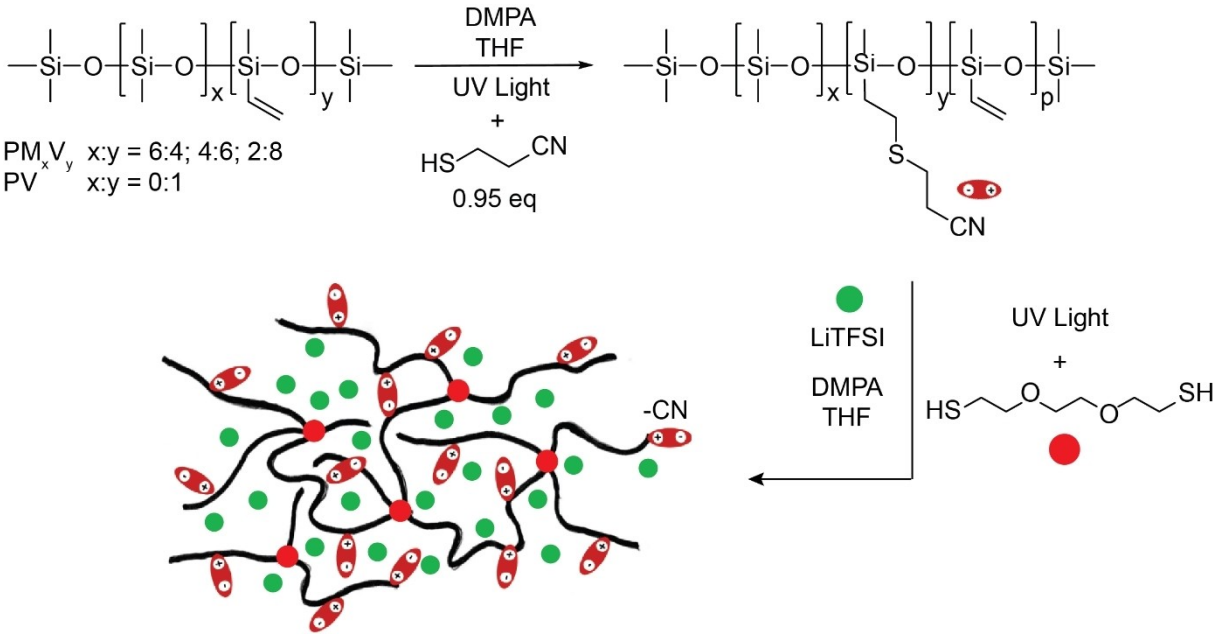

Figure 1. Schematics of the synthetic procedure of PSSEs.

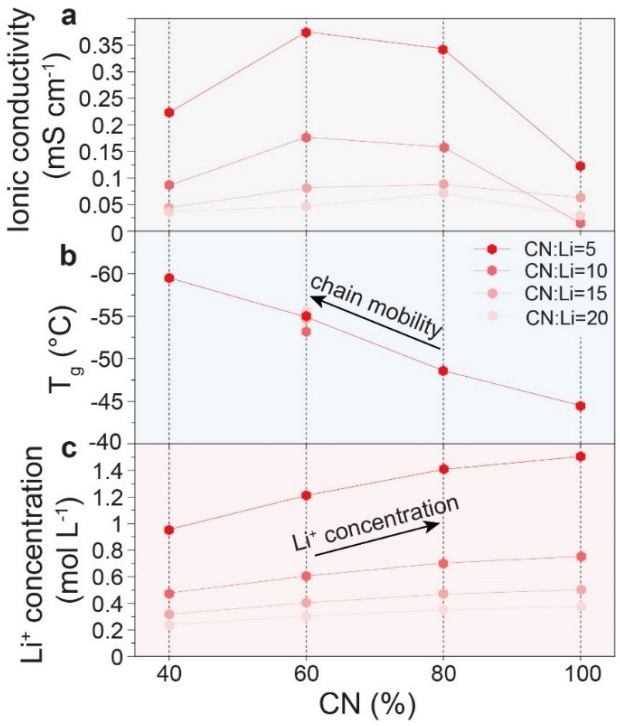

Figure 2. The comparison of ionic conductivity at 60 °C (a), glass transition temperature (T_g) (b) and Li^+ ion concentration (c) of PSSEs comprising different quantities of CN groups and CN:Li molar ratios.

CN:Li^+ < 5 resulted in highly viscous polymer solutions that could not be uniformly tape-casted.

Second, PSSEs with 40% and 100% CN groups, in general, showed lower ionic conductivity compared to 60% and 80% CN groups. This observation can be explained by the higher T_g of PSSEs with 100% CN group (Figure 2b, S1, and Table S2), which diminishes the ionic conductivity of PSSE with CN:Li^+ ratio of 5, due to poorer segmental motion and, therefore lower Li-ion mobility, compared to PSSEs containing 60% and 80% CN groups. Notably, T_g changes only marginally at different ratios of CN:Li^+, as evidenced in Figure 2b. Lower ionic conductivity of PSSEs with 40% CN groups was associated with the lowest Li^+ ion charge carrier concentration compared to the polymer compositions with higher CN content (Figure 2c).

To evaluate the ionic conductivity of PSSEs at elevated temperatures and consequently estimate their pseudo-activation energies, additional EIS measurements were conducted at different temperatures for polymers with different CN groups while maintaining a CN:Li^+ ratio of 5 (Figures 3a, S2, S3 and Table S3). The Arrhenius plot (Figure 3a) exhibited the typical non-linear behavior associated with polymer electrolytes, which can be described by the Vogel-Tammann-Fulcher (VTF) equation (eq. 1):[15]

$$\sigma = AT^{-1/2}e^{-B/k(T-T_0)} \quad (1)$$

where σ [S cm^{-1}] is the ionic conductivity in, A [S $K^{1/2}$ cm^{-1}] is a fitting constant proportional to the number of charge carriers, B [eV] is the pseudo-activation energy, k [J K^{-1}] is the Boltzmann constant and T_0[K] is the equilibrium temperature ($T_0 = T_g - 50$). According to Figure 3a, S3 and Table S3, the pseudo-activation energies of the PSSEs were determined to be very similar for all measured compositions at a level of *ca.* 0.1 eV.

Electrochemical Measurements

Considering that PSSE with 60% CN groups and a CN:Li ratio of 5 (PSSE-60-5) exhibited the highest ionic conductivity of 0.375 mS cm^{-1} at 60 °C and low pseudo-activation energy of *ca.* 0.1 eV, this polymer composition was chosen for the further electrochemical characterization, namely, the determination of the Li^+ ion transfer number, and cycle stability measurements in both symmetrical and full-cell configurations. To determine the Li^+ ion transfer number, impedance measurements were performed in Li/PSSE-60-5/Li symmetrical cell configuration followed by galvanostatic cycling at a low current density of 0.001 mA cm^{-2} (4 h of charge/ discharge), followed by a 30-minutes rest in-between each half-cycle for interface stabilization (6 cycles in total).[14] Subsequently, the cell was polarized with 10 mV *vs.* Li^+/Li for 10 h until a steady state current was reached, followed by a second impedance measurement (Figure 3b). The calculations of the transference number were performed using the Bruce-Vincent equation:[14,16]

$$T_{ss} = \frac{I_{ss}}{I_0} x \frac{(\Delta V - I_0 R_0)}{(\Delta V - I_{ss} R_{ss})} \quad (2)$$

where T_{ss} is the transference number, △V [V] is the applied potential, I_0 [Amp] and I_{ss} [Amp] are the initial and steady-state currents from the polarization measurement, R_0 [Ohm] and R_{ss} [Ohm] are initial and steady-state resistance from the impedance measurements, respectively.

The Li^+ ion transfer number of PSSE-60-5 was found to be 0.73, approaching that of a single ion conductor, which is one of the highest values reported to date for polymeric Li-ion conducting electrolytes.[5b,17] Although the functionalization of the PS backbone with a high CN content of 60% leads to an increase in the dielectric constant of the PS polymers,[18] the high Li^+ ion transfer number of PSSE-60-5 indicates rather weak dipolar interactions between Li^+ ions and CN-functionalized PS chains,[6b,19] in contrast to, for example, oxygen-containing backbones of polyethylene oxide-based Li-ion electrolytes.[20]

Next, the ability of the electrolyte to support reversible electrochemical lithium plating/stripping was studied through galvanostatic cycling measurements of Li/PSSE-60-5/Li symmetrical cells. These cells were prepared by pressing two symmetrically aligned Li disks on both sides of PSSE-60-5 polymer. The measurements were conducted under the pressure of 0.75 MPa at 60 °C using a homemade cell setup (Figure S4).

As an initial step, we targeted to determine the achievable critical current density (CCD) of the studied polymer, that is, the current density at which Li dendrite propagation begins.[21] The test was performed using galvanostatic cycling experiments at

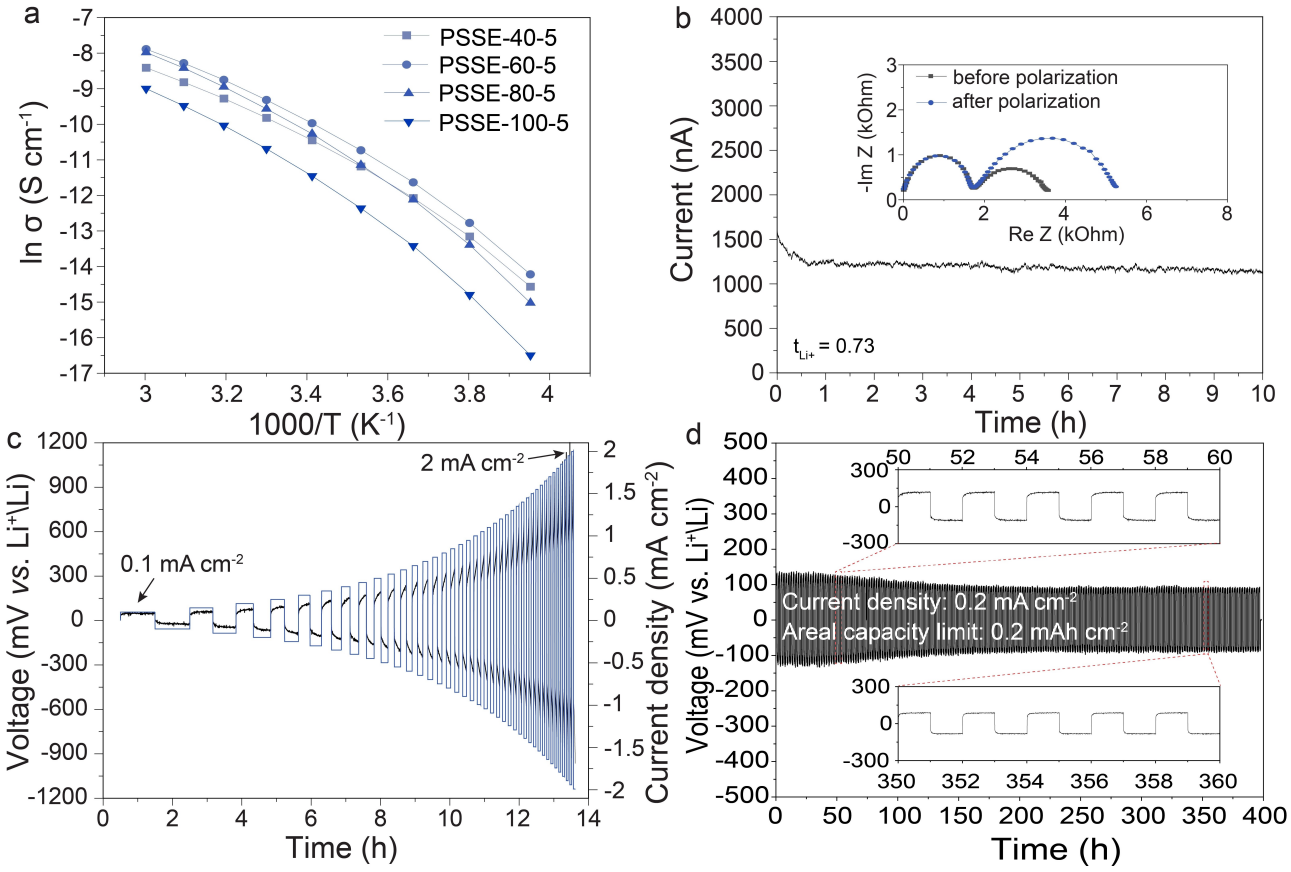

Figure 3. (a) Arrhenius plots of the measured total conductivity PSSEs comprising different quantities of CN groups (40, 60, 80, and 100%) at identical CN:Li molar ratio of 5. (b) Polarization measurements of PSSE-60-5 performed at 10 mV and the Nyquist plots measured before and after polarization. (c) Voltage profiles of Li/PSSE-60–5/Li symmetrical cells, measured at different current densities ranging from 0.1 mA g^{-1} to 2 mA g^{-1} with a capacity limitation of 0.1 mAh cm^{-2} per half-cycle. (d) Voltage profiles of Li/PSSE-60-5/Li symmetrical cell, measured at a current density of 0.2 mA cm^{-2} with capacity limitation of 0.2 mAh cm^{-2} per half-cycle. The measurements shown in (c) and (d) were conducted at 60 °C applying uniaxial pressure of *ca.* 0.75 MPa.

different current densities. Specifically, the current density was increased from 0.1 mA cm^{-2} in increments of 0.05 mA cm^{-2}, carrying 0.1 mA h cm^{-2} of lithium for each half cycle (Figure 3c). Notably, no short circuit was observed for the symmetric cell up to 2 mA cm^{-2} current rate, where the measurements had to be terminated owing to prohibitively high overpotential. This result shows that PSSE-60-5 can sustain efficient lithium-ion transport even at high current densities and yet at low pressure and moderate temperatures.

The cycling stability of the prepared symmetrical cell was then assessed through additional electrochemical measurements at a constant current density of 0.2 mA cm^{-2} and a limiting areal capacity of 0.2 mA h cm^{-2} per half cycle. As shown in Figure 3d, the Li/PSSE-60-5/Li cells exhibited high cycling stability up to 400 h, corresponding to 80 mAh cm^{-2} of cumulative lithium areal capacity. Importantly, the cells exhibited a stable overpotential of ~100 mV throughout the cycling measurements.

The potential of polymer as a Li-ion solid-state electrolyte was evaluated in the cell comprising LFP-PSSE-60-5 cathode composites (catholytes) and lithium metal anode. The catholytes were prepared by mixing $LiFePO_4$ (LFP, 65 wt%) as active material and carbon black (10 wt%) as an electronic conductive additive in an agate mortar, followed by their mixing with polymeric solution (25 wt%) serving as both binder and ion-conducting medium. The polymer solution was prepared by mixing PS-based polymer functionalized with 60% CN groups, LiTFSI salt (CN:Li^+ ratio of 5), cross-linker (10 vol% in N-methyl-2-pyrrolidone (NMP)), and thermal initiator (azobisisobutyronitrile) dissolved in NMP. The well-mixed slurry was then tape-cast on a carbon-coated aluminum foil current collector using a 100 μm blade opening. Afterwards, the tape was dried at 80 °C under air to evaporate the solvent and then at 100 °C under vacuum for thermal crosslinking. A photograph of a highly uniform layer of the polymer cathode composite is shown in Figure S6.

Full-cells were prepared by stacking the discs of lithium metal anode, PSSE-60-5 polymer electrolyte separator, and catholyte. A cross-section Scanning Electron Microscopy (SEM) image of a full-cell stack (Figure 4a), together with Energy Dispersive X-ray Spectroscopy (EDX) elemental analysis of the polymer cathode composite demonstrated the uniform distribution of PSSE-60-5 and LFP (Figure 4b, d, and e). The homogeneous distribution of PSSE-60-5 in the cathode composite is the key factor in sustaining an effective Li^+ ion transport to the active materials within the catholyte.

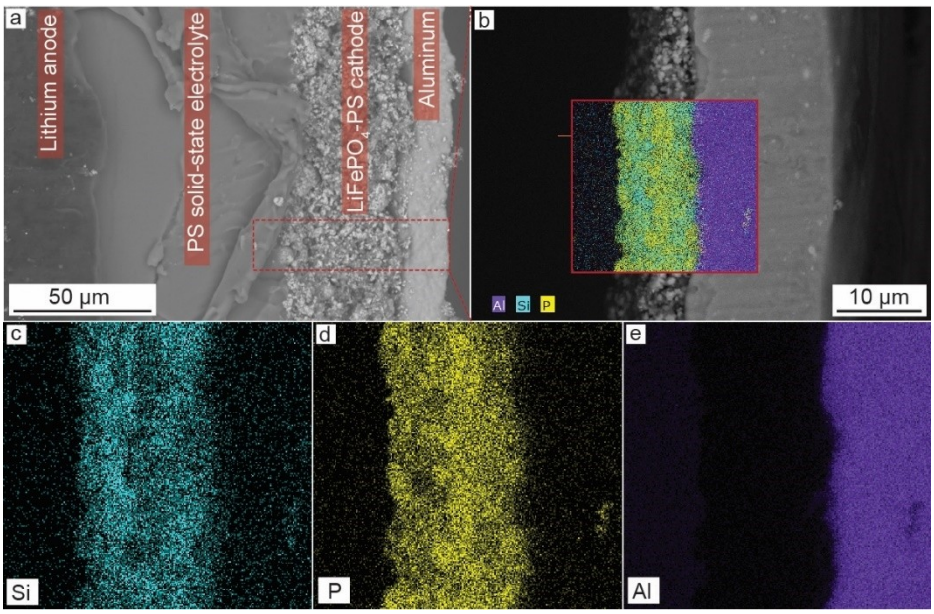

Figure 4. (a) Cross-sectional SEM image and (b) EDX elemental map of a full-cell comprising lithium anode, PSSE-60-5, $LiFePO_4$-PSSE-60-5 cathode, and Al current collector. Individual EDX maps of Si (c), P (d) and Al (e) measured on PSSE-60-5/$LiFePO_4$-PSSE-60-5/Al cross section (shown as red square in (b)). The cross-sectional images of the full-cell after electrochemical cycling are shown in Figure S5.

Prior to assessing the electrochemical performance of the full-cells based on the developed polymer, we evaluated its oxidation electrochemical stability at 60 °C by cyclic voltammetry measurement between 0.5–4.2 V *vs.* Li^+/Li with a scan rate of 1 mV s^{-1} (Figure 5a). The cells were prepared by placing PSSE-60-5 in between symmetrically aligned carbon-coated

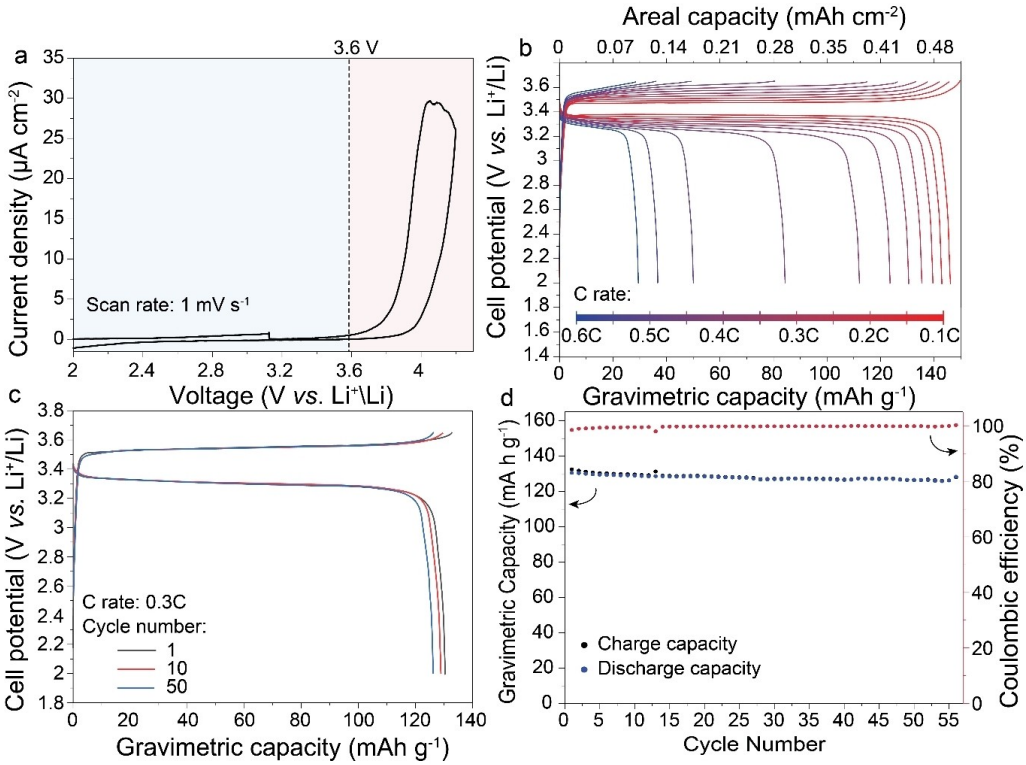

Figure 5. (a) Cyclic voltammetry curves of PSSE-60-5 measured in Li/PSSE-60-5/stainless steel configuration at a scan rate of 1 mV s^{-1}. Galvanostatic charge/discharge voltage profiles of Li/PSSE-60-5/LFP-PSSE-60-5 full-cell measured at different C rates ranging from 0.1 C to 0.6 C (b) and at 0.3 C rate for cycle numbers of 1, 10 and 50 (c). (d) Cycling stability measurements of Li/PSSE-60-5/LFP-PSSE-60-5 full-cell at 0.3 C. The measurements shown in (b), (c), and (d) were conducted at 60 °C applying uniaxial pressure of ca. 0.75 MPa. The electrochemical performance of the full-cells based on other PPSEs with different nitrile groups and CN:Li^+ ratios can be found in Figure S7.

aluminum foil and lithium foil as working and counter/reference electrodes, respectively. It was determined that the onset of electrochemical oxidation occurs at *ca.* 3.7 V *vs.* Li^+/Li and therefore slightly lower voltage of 3.65 V *vs.* Li^+/Li was selected as an upper potential limitation for full-cell measurements.

The performance of PS-based solid-state Li batteries under real working conditions was assessed by conducting galvanostatic cycling at various C rates ranging from 0.1 C (0.06 mA cm^{-2}) to 0.6 C (1.02 mA cm^{-2}), Figure 5b. LFP can be reversibly de-lithiated and lithiated at *ca.* 3.5 and 3.4 V *vs.* Li^+/Li, respectively, delivering a high storage capacity of 148 mAh g^{-1} (*ca.* 90% from the theoretical capacity of 165 mAh g^{-1}) at low C rate of 0.1 C. At higher C rates, the discharged capacity drops to 139, 130, 112, 50, and 30 mA h g^{-1} at 0.2, 0.3, 0.4, 0.5, and 0.6 C, respectively. We hypothesize that the poor rate capability might stem from insufficient electronic percolation in the LFP cathode, requiring further optimization, for instance, by employing CNT as an electron conductive additive due to its high aspect ratio. The cycling stability test of full-cells employing PSSE-60-5, performed at 0.3 C rate, showed high capacity retention of LFP cathode of 97% over 50 cycles (Figure 5c, d) with a high Coulombic efficiency of *ca.* 99.65%.

Conclusions

In this work, we have thoroughly investigated the influence of nitrile group content and CN:Li^+ ratio on the ionic conductivity of PS polymers. Side-by-side characterization of the synthesized PS polymers by EIS, differential scanning calorimetry, and dielectric permittivity measurements revealed that, on the one hand, incorporation of nitrile groups into the PS backbone increases the dielectric permittivity and thus promotes the LiTFSI solvation in the PS polymer, and increases charge carrier concentration of the Li^+ ions. On the other hand, an increase in the CN content leads to an increase in the glass transition temperature, lowering chain mobility, which has a negative effect on the Li-ion charge carrier mobility. Another important aspect concerned the processability of the PS polymers. While a decrease in the CN:Li^+ ratio fosters enhancement in ionic conductivity of the PS polymers due to an increased concentration of Li^+ charge carriers, a CN:Li^+ ratio below 5 leads to the formation of viscous polymer solutions that are unsuitable for the fabrication of uniform coatings *via* tape casting.

Among the different synthesized PSSE compositions, the highest ionic conductivity of 0.375 mS cm^{-1} at 60 °C was found for the PS polymer with 60% CN groups and a CN:Li^+ ratio of 5 (PSSE-60-5). The Li^+ ion transfer number was as high as 0.73, indicating rather weak dipolar interactions between Li^+ ions and the polymer chain with CN groups. Importantly, the developed PSSE-60-5 in a symmetric Li/PSSE-60–5/Li cell configuration exhibited a high CCD of up to 2 mA cm^{-2} and a long cycling stability of up to 400 h at a current density of 0.2 mA cm^{-2} and an area capacity limit of 0.2 mAh cm^{-2}. The electrochemical performance of PSSE-60-5 was also investigated with an LFP cathode. Li/PSSE-60-5/LFP full-cells demonstrated a high initial gravimetric charge storage capacity of about 132 mAh g_{LFP}^{-1} and about 100% of this capacity was maintained for 55 cycles at 0.3 C rate.

Experimental Section

Chemicals

1,3,5,7-Tetramethyl-1,3,5,7-tetravinyl cyclotetrasiloxane (V4, ABCR), hexamethyldisiloxane (98%, ABCR), octamethylcyclotetrasiloxane (D4, 97%, ABCR), 2,2-dimethoxy-2-phenylacetophenone (DMPA, Merck), calcium hydrate (Merck), aqueous solution of tetramethylammonium hydroxide (TMAH, 25 wt%, Merck), anhydrous benzene (Merck), methanol (Merck), tetrahydrofuran (THF, Merck), chloroform (Merck), magnesium sulfate (Merck), sodium hydroxide (Merck), 3-chloropropionitrile (Merck), thiourea (Merck), sulfuric acid (Merck), 2,2′-(ethylenedioxy) diethanethiol and azobisisobutyronitrile (Sigma Aldrich) were of reagent grade and used as received without purification. 2-Cyanoethanethiol was synthesized according to the literature.[22] Carbon black (CB, Super P, IMERYS), 3 wt% carbon-coated $LiFePO_4$ (LFP, Aleees), N-methyl-2-pyrrolidone (NMP, Thermo Fisher Scientific) were used as received.

Synthesis of polysiloxanes

PM_xV_y and PV were synthesized according to previous report.[18]

Synthesis of polysiloxanes functionalized with nitrile groups

In a typical synthesis, 20 g of PM_xV_y or PV viscous polysiloxane polymers were dissolved in 600 ml of THF, followed by the addition of 2-cyanoethylthiol (28.8 g, 0.331 mole, 0.95 equiv. to reactive vinyl groups) and DMPA (0.846 g, 0.009 equiv. to reactive vinyl groups). The reaction mixture was degassed three times using the freeze-pump-thaw technique and then irradiated for 20 min with a UV light. The reaction of thiol with vinyl groups yielded the polymers functionalized with nitrile groups. The amount of the vinyl-group was defined by molar ratio between non- and vinyl-group containing repeating units (dimethylsiloxane/methylvinylsiloxane = 6:4; 4:6; 2:8 and 0:1). Considering that *ca.* 5% of vinyl side groups were subsequently used for crosslinking, the quantity of 2-cyanoethanethiol was adjusted to *ca.* 0.95 equivalent per vinyl group present in PM_xV_y or PV. Then, the solution was heated in a rotary evaporator to increase the concentration of the functionalized PM_xV_y/PV. Afterwards, the polymer was washed four times by dissolution/precipitation in THF/methanol and dried at room temperature for *ca.* 24 h. The concentration of THF in the dried polymer was *ca.* 5–2 wt%. Complete drying was avoided to prevent undesired reactions between remaining vinyl groups. Importantly, the completeness of the reaction between thiol and vinyl groups was confirmed by Raman spectroscopy measurements (see Figure S8). Raman Spectroscopy measurements were performed using a confocal Raman microscope (Horiba, LabRAM HR Evolution) equipped with an Nd:Yag 532 nm laser (Cobolt SambaTM).

Preparation of PSSE

PSSEs were prepared by the addition of different amounts of LiTFSI salt in the synthesized polymers, corresponding to the CN:Li^+ molar ratio of 20, 15, 10, or 5. Afterwards, DMPA and 2,2′-(ethylenedioxy) diethanethiol as photoinitiator and cross-linker (CL), respectively, were added to the polymer slurry. The obtained mixture was blade coated on a Teflon substrate with 250 μm blade opening at a speed of 1 mm s^{-1}, followed by UV crosslinking for *ca.* 5 minutes. Cross-

linked polymer films were then peeled off from the substrate, cut into small 6 mm discs, and vacuum dried in antechamber at 60 °C overnight for further use. The thickness of the fabricated Li-ion electrolyte discs was intentionally set at 110 μm, as shown in Figure S9. However, it is important to note that it was entirely feasible to produce thinner or thicker variants of the electrolyte, as illustrated in Figure S10. The prepared electrolytes were denoted as PS–X-Y (see Table S1), where X indicates the percentage of the repeating units that are functionalized with CN groups (40, 60, 80, or 100 %) and Y refers to the CN:Li^+ ratio (20, 15, 10, or 5). Stress-strain data for prepared PSSEs are shown in Figure S11. Compression tests were conducted using Tinius Olsen Universal Testing Machine at a loading rate of 1 μm s^{-1}. The flexibility of the prepared PSSEs is demonstrated in Video S1.

SEM and EDX measurements

SEM and EDX analysis were performed using Hitachi TM3030Plus Tabletop SEM with an acceleration voltage of 10 kV.

DSC measurements

DSC measurements were conducted using Perkin Elmer DSC8000 device between the temperatures of −100 °C and 50 °C with a heating and cooling rate of 10 °C min^{-1} under constant N_2 flow. On average, 9.5 mg samples were used for the measurements. Figure S1 shows the first heating curve.

Measurements of the ionic conductivity and electrochemical stability window

The ionic conductivity of polymers was assessed by EIS measurements. Corresponding polymer electrolytes were cut into discs (diameter = 8 mm), dried under vacuum at 60 °C overnight, and placed between two stainless steel current collector discs inside the coin-type cell (316 L, Hohsen Corp) for EIS measurements. Coin-type cells were assembled in a glovebox under argon atmosphere (< 0.1 ppm H_2O/O_2). The thickness of the polymer placed between current collector discs was measured using a digital thickness gauge (Brütsch-Rüegger Mitutoyo). EIS measurements were performed in the frequency range from 10 Hz to 3.5×10^7 Hz with an amplitude of 0.01 V within a temperature range of −20 °C to 60 °C, using Biologic MTZ-35 impedance analyzer, ITS-e enhanced intermediate temperature system.

The electrochemical stability window of prepared Li-ion conducting polymers was assessed by cyclic voltammetry measurements performed in coin-type cells assembled in a glovebox under an argon atmosphere (< 0.1 ppm H_2O/O_2). The cells consisted of lithium foil as the counter and the reference electrode, carbon-coated aluminum foil as a working graphite electrode, and a Li-ion conducting polymer placed between both electrodes. The measurements were performed within a voltage range of 0.5 V–4.2 V *vs.* Li^+/Li with a speed of 1 mV s^{-1} at 60 °C using Biologic VMP3 potentiostat/galvanostat.

Transference number measurement

A lithium symmetric coin-type cell is assembled in the glovebox with the configuration of Li/PSSE-60-5/Li. First, impedance measurement is done in the frequency range from 10 Hz to 10^7 Hz with an amplitude of 0.01 V, using Biologic SP-150 multifunctional potentiostat/galvanostat. Then, the symmetric cell is galvanostatically cycled at 0.001 mA cm^{-2} current rate (4 hours of charge/discharge), followed by 30 minutes rest between each half cycle for 6 cycles. Afterwards, the symmetric cell is polarized to 10 mV *vs.* Li^+/Li until reaching a steady-state current for 10 hours. After the polarization, the second impedance measurement is performed. All measurements were performed at 60 °C.

Preparation of polymer cathode composite

3 wt% carbon-coated $LiFePO_4$ (0.13 g) and carbon black (0.02 g) powders were ground in an agate mortar for 5 minutes. Afterwards, Li-conducting polysiloxane polymer solution (0.05 g) was added to the obtained $LiFePO_4$/carbon black mixture, followed by its further grounding for 15 min. The polymer solution was prepared by dissolving Li-conducting polysiloxane polymer (PS-60, non-cross-linked), 2,2′-(ethylenedioxy) diethanethiol cross-linker (29 μL, 10 vol.% in NMP) and azobisisobutyronitrile thermal initiator (29 μL, 10 vol.% in NMP) in NMP solvent. The obtained slurry was then tape-cast on a carbon-coated aluminum foil current collector via doctor-blading (gap: 100 μm), at a speed of 1 mm s^{-1}. The obtained cathode tape was first dried shortly at room temperature followed by drying at 80 °C under air and then at 100 °C under vacuum to thermally crosslink the polymer. The polymer cathode was additionally dried overnight at 80 °C under vacuum in an antechamber of an argon-filled glovebox prior to being used for battery assembly.

Symmetric and full-cell preparation

Li/PSSE-60-5/Li symmetric cells were prepared by placing symmetrically alighted lithium discs (d = 6 mm) onto polymer Li-ion electrolyte discs (d = 8 mm). Electrochemical measurements were performed at 60 °C under 0.75 MPa pressure inside an Ar-filled glovebox. Full-cells were prepared by placing PSSE-60-5 (d = 8 mm) in between two symmetrically aligned lithium metal anode (d = 6 mm) and LFP polymer cathode (d = 6 mm) and then cycled at 60 °C under pressure of 0.75 MPa inside of the Ar-filled glovebox. The electrochemical measurements of full-cells were performed using a multichannel workstation Biologic VMP3 in the voltage window of 2–3.65 V *vs.* Li^+/Li. The electrochemical performance of the cells at the higher upper voltage of 3.7 V *vs.* Li^+/Li is shown in the Figure S12.

Author Contributions

D.M.O, M.V.K. and K.V.K. conceived and supervised the project. M.I. conducted the first preliminary experiments on the Li-ion conductivity of different electrolytes. Y.S. conducted the synthesis of polymers. F.O. manufactured and characterized the batteries with support from C.Z., P.H., Y.S., H.Z., and A.F. The SEM measurements were conducted by F.O. F.O., K.V.K and M.V.K. wrote the paper with input from all authors. All authors contributed to discussions and gave the approval for the final version of the manuscript.

Acknowledgements

The authors thank Matthias Klimpel for his help on VTF calculations. D.M.O. gratefully acknowledges the funding from the European Research Council (ERC) under the European Union's Horizon 2020 research and innovation program (grant agreement No. 101001182), the financial support of Swiss

National Science Foundation (IZERZO_142215 and 200020_172693), funding from Empa, the Swiss Federal Laboratories for Materials Science and Technology, through an internal research call. M.I. acknowledges the financial support from the European Union's Horizon 2020 research and innovation program under the Marie Skłodowska-Curie grant agreement number 754364.

Conflict of Interests

The authors declare no conflict of interest.

Data Availability Statement

The data that support the findings of this study are available from the corresponding author upon reasonable request.

Keywords: poly (siloxane) · nitrile-functionalized · solid electrolyte · lithium metal batteries

[1] a) J. W. Wen, Y. Yu, C. H. Chen, *Mater. Express* **2012**, *2*, 197–212; b) J. H. Li, Y. F. Cai, H. M. Wu, Z. Yu, X. Z. Yan, Q. H. Zhang, T. D. Z. Gao, K. Liu, X. D. Jia, Z. N. Bao, *Adv. Energy Mater.* **2021**, *11*, 2003239; c) R. Y. Fang, B. Y. Xu, N. S. Grundish, Y. Xia, Y. T. Li, C. W. Lu, Y. J. Liu, N. Wu, J. B. Goodenough, *Angew. Chem. Int. Ed.* **2021**, *60*, 17701–17706.

[2] C. Berthier, W. Gorecki, M. Minier, M. B. Armand, J. M. Chabagno, P. Rigaud, *Solid State Ionics* **1983**, *11*, 91–95.

[3] a) B. Sun, J. Mindemark, K. Edstrom, D. Brandell, *Solid State Ionics* **2014**, *262*, 738–742; b) J. J. Zhang, J. F. Yang, T. T. Dong, M. Zhang, J. C. Chai, S. M. Dong, T. Y. Wu, X. H. Zhou, G. L. Cui, *Small* **2018**, *14*, 1800821.

[4] a) P. M. Blonsky, D. F. Shriver, P. Austin, H. R. Allcock, *Solid State Ionics* **1986**, *18(9)*, 258–264; b) N. Kaskhedikar, J. Paulsdorf, A. Burjanadze, Y. Karatas, B. Roling, H. D. Wiemhofer, *Solid State Ionics* **2006**, *177*, 2699–2704.

[5] a) Z. C. Zhang, D. Sherlock, R. West, R. West, K. Amine, L. J. Lyons, *Macromolecules* **2003**, *36*, 9176–9180; b) Q. L. Wang, H. R. Zhang, Z. L. Cui, Q. Zhou, X. H. Shangguan, S. W. Tian, X. H. Zhou, G. L. Cui, *Energy Storage Mater.* **2019**, *23*, 466–490.

[6] a) R. Hooper, L. J. Lyons, M. K. Mapes, D. Schumacher, D. A. Moline, R. West, *Macromolecules* **2001**, *34*, 931–936; b) M. Grunebaum, M. M. Hiller, S. Jankowski, S. Jeschke, B. Pohl, T. Schurmann, P. Vettikuzha, A. C. Gentschev, R. Stolina, R. Muller, H. D. Wiemhofer, *Prog Solid State Ch* **2014**, *42*, 85–105; c) Y. L. Hu, X. X. Xie, W. Li, Q. Huang, H. Huang, S. M. Hao, L. Z. Fan, W. D. Zhou, *Acs Sustain Chem Eng* **2023**.

[7] a) J. E. Companik, S. A. Bidstrup, *Polymer* **1994**, *35*, 4823–4833; b) S. Zhao, Y. M. Zhang, H. Pham, J. M. Y. Carrillo, B. G. Sumpter, J. Nanda, N. J. Dudney, T. Saito, A. P. Sokolov, P. F. Cao, *ACS Appl. Energ. Mater.* **2020**, *3*, 12540–12548; c) X. Y. Zhang, J. Y. Dai, M. Tepermeister, Y. Deng, J. J. Yeo, M. N. Silberstein, *Macromolecules* **2023**, *56*, 3119–3131.

[8] a) I. M. Khan, Y. X. Yuan, D. Fish, E. Wu, J. Smid, *Macromolecules* **1988**, *21*, 2684–2689; b) C. P. Fonseca, S. Neves, *J. Power Sources* **2002**, *104*, 85–89.

[9] a) J. Li, Y. Lin, H. H. Yao, C. F. Yuan, J. Liu, *ChemSusChem* **2014**, *7*, 1901–1908; b) U. H. Choi, S. W. Liang, Q. Chen, J. Runt, R. H. Colby, *Acs Appl Mater Inter* **2016**, *8*, 3215–3225.

[10] a) Y. Karatas, N. Kaskhedikar, M. Burjanadze, H. D. Wiemhofer, *Macromol. Chem. Phys.* **2006**, *207*, 419–425; b) J. Shim, L. Kim, H. J. Kim, D. Jeong, J. H. Lee, J. C. Lee, *Polymer* **2017**, *122*, 222–231; c) J. Shim, J. W. Lee, K. Y. Bae, H. J. Kim, W. Y. Yoon, J. C. Lee, *ChemSusChem* **2017**, *10*, 2274–2283.

[11] a) S. S. Wang, K. Min, *Polymer* **2010**, *51*, 2621–2628; b) H. P. Liang, M. Zarrabeitia, Z. Chen, S. Jovanovic, S. Merz, J. Granwehr, S. Passerini, D. Bresser, *Adv. Energy Mater.* **2022**, *12*.

[12] K. H. Min, D. B. Kim, Y. K. Kang, D. H. Suh, *J. Appl. Polym. Sci.* **2008**, *107*, 1609–1615.

[13] I. J. Lee, G. S. Song, W. S. Lee, D. H. Suh, *J. Power Sources* **2003**, *114*, 320–329.

[14] C. Y. Fu, M. Iacob, Y. Sheima, C. Battaglia, L. Duchene, L. Seidl, D. M. Opris, A. Remhof, *J. Mater. Chem. A* **2021**, *9*, 11794–11801.

[15] S. H. Chung, K. Such, W. Wieczorek, J. R. Stevens, *J Polym Sci Pol Phys.* **1994**, *32*, 2733–2741.

[16] J. Evans, C. A. Vincent, P. G. Bruce, *Polymer* **1987**, *28*, 2324–2328.

[17] a) J. D. Zhu, Z. Zhang, S. Zhao, A. S. Westover, I. Belharouak, P. F. Cao, *Adv. Energy Mater.* **2021**, *11*; b) D. Chen, Y. Liu, C. Feng, Y. He, S. Zhou, B. Yuan, Y. Dong, H. Xie, G. Zeng, J. Han, W. He, *Electron* **2023**, *1*, e1.

[18] Y. Sheima, Y. Yuts, H. Frauenrath, D. M. Opris, *Macromolecules* **2021**, *54*, 5737–5749.

[19] a) W. H. Hou, C. Y. Chen, *Electrochim. Acta* **2004**, *49*, 2105–2112; b) S. Y. Xie, A. Nikolaev, O. A. Nordness, L. C. Llanes, S. D. Jones, P. M. Richardson, H. B. Wang, R. J. Clement, J. R. de Alaniz, R. A. Segalman, *Macromolecules* **2022**, *55(13)*, 5723–5732.

[20] a) K. Pozyczka, M. Marzantowicz, J. R. Dygas, F. Krok, *Electrochim. Acta* **2017**, *227*, 127–135; b) Y. Zhao, L. Wang, Y. A. Zhou, Z. Liang, N. Tavajohi, B. H. Li, T. Li, *Adv. Sci.* **2021**, *8*, 2003675.

[21] J. Liu, H. Yuan, H. Liu, C. Z. Zhao, Y. Lu, X. B. Cheng, J. Q. Huang, Q. Zhang, *Adv. Energy Mater.* **2022**, *12*, 2100748.

[22] R. Gerber, *Organic Synthesis, vols* **2000**, *10*, 234.

Manuscript received: August 30, 2023
Revised manuscript received: November 30, 2023
Accepted manuscript online: December 5, 2023
Version of record online: December 14, 2023